ChemPubSoc Europe

DOI: 10.1002/open.201600028

Open Access ChemistryOPEN Communications

Immobilization of Cellulase on Magnetic Nanocarriers

Hans-Christian Roth[+], Sebastian P. Schwaminger[+], Fei Peng, and Sonja Berensmeier*[a]

The constant increase in the number of sustainable products on the global markets demands new biotechnological processing strategies such as the purification and recovery of biocatalysts. Superparamagnetic iron oxide nanoparticles exhibit excellent recovery properties as carrier materials in enzyme catalysis. We present the simple and fast electrostatic assembly of cellulase (CEL) and low-priced silica-coated magnetic nanoparticles, which demonstrates stable enzyme bonding and excellent colloidal stability. The high CEL loading (0.43 $g\,g^{-1}$), without leaching of biocatalyst and high recovery yields (75%), could be sustained over ten magnetic recycling steps. The highlight of this study is the preservation of a high enzymatic activity and, therefore, the outstandingly high lifecycle stability.

With global warming and dwindling fossil fuel resources, the demand for sustainable energy has been increasing worldwide. A promising possibility for the production of biofuels is the application of biocatalysts for the conversion of regenerative feedstocks.[1] One of the most abundant biological raw materials is cellulose, which can be transformed into bioethanol via disintegration of the polysaccharide to glucose and subsequent alcoholic fermentation. The industrial implementation of biocatalysts is still in its infancy, owing to high production and operation costs. Hence, enzyme immobilization has high economic and ecologic potential in the development of sustainable and green bioprocesses.[2–6]

To date, only a few industrial applications of immobilized enzymes exist. One example is the isomerization of glucose to fructose by immobilized glucose isomerase, which is already processed industrially.[2] Other processing strategies beside fixed bed reactors, such as fluidized bed reactors, simulated moving bed reactors, and reactors with two impinging jets, are being investigated for glucose isomerase; however, no industrially applied process currently exists for high-molecular-weight cellulose hydrolysis with immobilized cellulase.[2] An interesting possibility for the implementation of such a process is the concept of the magnetically stabilized bed reactor (MSBR), which is already used for lipase immobilized on magnetic nanoparticles (MNPs).[7,8] In a MSBR, the principle of high-gradient magnetic separation, where a magnetic field is applied perpendicularly to the process stream, is used to recover the catalyst immobilized on MNPs.

Following this trend of developing appropriate enzyme recovery techniques for cost reduction in biocatalytic processes, numerous immobilization strategies for enzymes have been reported.[4,9] Typical strategies for immobilization are noncovalent adsorption, ionic interaction, covalent binding, the cross-linking of enzymes, and encapsulation in gels or capsules.[10]

The accessibility of the substrate to the active center is a bottleneck in enzyme technology.[6] Most immobilization methods for enzymes in porous microcarrier materials and gel capsules demonstrate diffusion limitations.[10] On the other hand, cross-linked or covalently bound enzymes often encounter comparable accessibility problems, owing to steric hindrance of active sites.[5,11] Although immobilization on or inside microcarriers is usually used for the heterogenization of homogeneous catalysts, enzymes on nanocarriers can be described as pseudo-homogeneous systems that are able to circumvent accessibility problems.[7,12,13]

For new process designs, magnetic nanoparticles are of special interest, as they can be manipulated by a magnetic field and, therefore, enable an easy recycling and separation method for catalysts and biomolecules from high viscous liqueurs and high-solid-content broths.[7,12,14] Iron oxide nanoparticles, which demonstrate superparamagnetic behavior, are nontoxic particles that can be synthesized cost-effectively through the co-precipitation of iron salts.[12,15] Silica coating is often used to stabilize magnetic particles in colloidal suspensions, as the coating strongly affects the surface charge.

Here, we present an effective enzyme carrier system based on superparamagnetic iron oxide nanoparticles, which can be recycled and reused multiple times without loss of enzymatic activity. In this context, Roth et al. have demonstrated an excellent separation efficiency and recovery in highly viscous process media of similar nanoparticles with a high-gradient magnetic separator.[16]

The focus of this investigation is the adsorption behavior and the resulting enzymatic activity of cellulase (CEL) on two different nanoparticle surfaces. Hence, we try to understand the impact of the nanoparticle surface properties on the surrounding protein corona for two industrially applicable bio-nano systems. The synthesis of MNPs, the silica coating, the CEL immobilization, and the enzymatic process are illustrated in Scheme 1.

MNPs with defined and optimized physical properties were synthesized by using a simple co-precipitation route based on the Massart process.[15] Transmission electron microscopy (TEM)

[a] H.-C. Roth,[+] S. P. Schwaminger,[+] F. Peng, Prof. S. Berensmeier
Technical University of Munich
Boltzmannstraße 15, 85748 Garching bei München (Germany)
E-mail: S.Berensmeier@tum.de

[+] These authors contributed equally to this work

Supporting Information for this article can be found under http://dx.doi.org/10.1002/open.201600028.

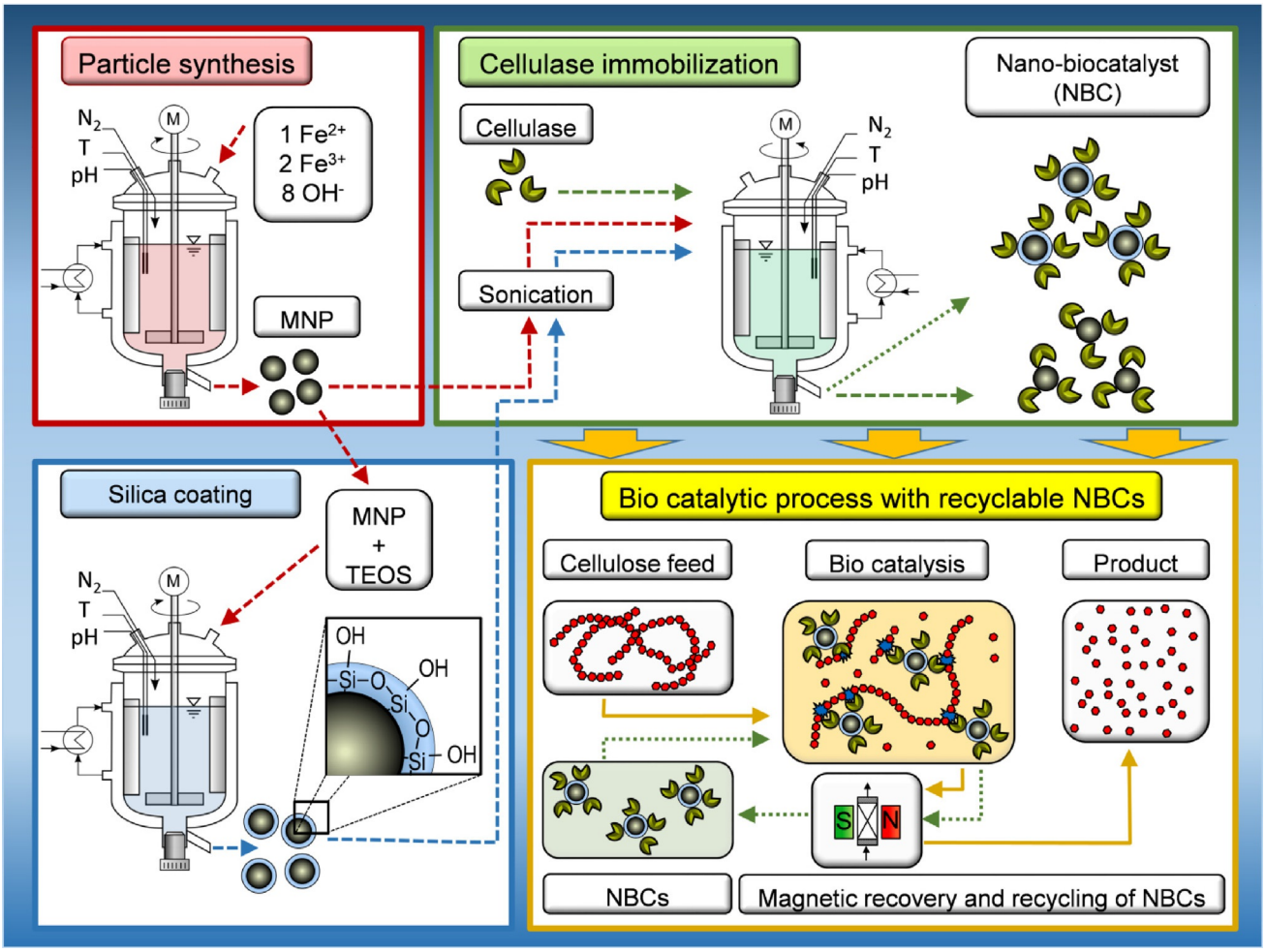

Scheme 1. Schematic description of particle synthesis (red frame), silica coating (blue frame), cellulase immobilization (green frame), and the biocatalytic process with recyclable NBCs (yellow).

data (Figure 1 a) indicate a particle-size distribution with a low dispersity and an average diameter of 11 nm. TEM measurements can be verified by X-ray diffraction (XRD) (Figure S1). Approximation of the XRD data with the Scherrer equation yields an average particle diameter of 10 nm. The MNPs were further coated with silica through the Stöber process, utilizing tetraethyl orthosilicate (TEOS) as a precursor. Optimization of the process with respect to the TEOS dosing rate, temperature, stirring speed, as well as concentration and ratio of MNPs to TEOS yielded a uniform silica shell with a thickness of 2 nm (Figure 1 b). The presence of a silica shell was evidenced by X-ray photoelectron spectroscopy (XPS) (Figures S2 and S3). Furthermore, a strong Si–O(Si) antisymmetric stretch vibration band at 1080 cm^{-1} was observed by using attenuated total reflection infrared spectroscopy (ATR–IR) (Figure S4).[17] Moreover, the specific surface area was determined by nitrogen adsorption isotherms and is in a similar range for the MNPs (99 $m^2 g^{-1}$) and silica-coated MNPs (MNP@SiO) (116 $m^2 g^{-1}$).

Surface modification with a silica coating shifts the point of zero charge (PZC) from pH 7.8 for uncoated MNPs to pH 4.6 (Figure S5). This leads to a negative charge for MNP@SiO in the pH range from 5 to 8, which is optimal for the highest enzymatic activity for most CEL species.[11] The zeta potential shifts even more significantly than the PZC into a negative region and emphasizes the change of electrostatic surface properties upon coating (Figure S6 a). CEL from Trichoderma longibrachiatum (EC 3.2.1.4) exhibits an isoelectric point (IEP) of 4.9.[11] Hence, at pH 5, MNP@SiO and CEL are almost uncharged, whereas the charge of uncoated MNPs is positive. Therefore, a much stronger electrostatic interaction is suspected for the immobilization of CEL on uncoated particles. Thus, the binding affinity and maximum load (q_{max}) do not diverge significantly (Figure 2). This behavior can be explained by stronger hydrophobic interactions of the MNP@SiO, which can result in different binding domains of the CEL and, therefore, different enzyme activities. The CEL binding affinity and q_{max} values were screened from pH 4 to 8. The best conditions were found at pH 5, and no influence of the incubation time between 5 min and 24 h was detected. The influence of temperature on the binding affinity and q_{max} was investigated from 20 to 60 °C at pH 5. Optimal conditions of 50 °C at pH 5 were employed for further CEL immobilization experiments. Adsorption isotherms were investigated through photometric analysis of the supernatant under equilibrium conditions. Sonication of the

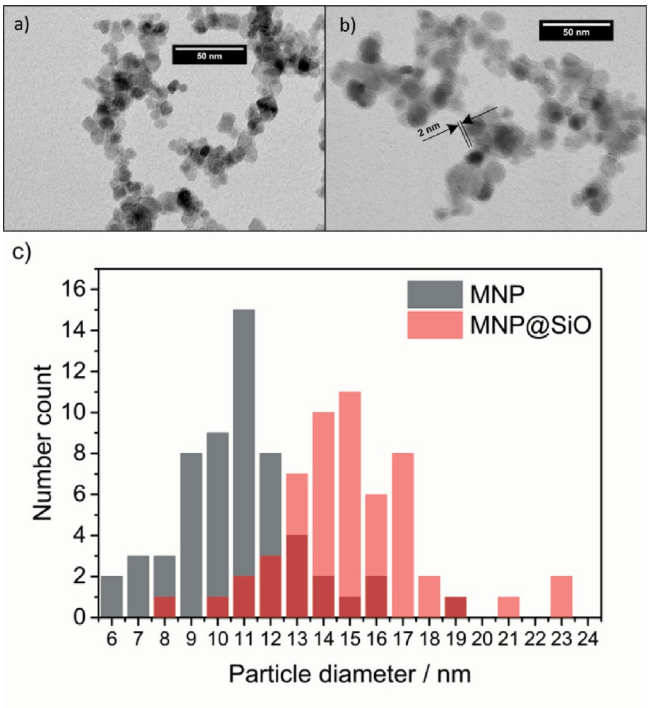

Figure 1. a) TEM image of the synthesized MNPs. b) TEM image of MNP@SiO with a 2 nm silica shell. c) Particle-size distribution as function of the number count from the TEM data.

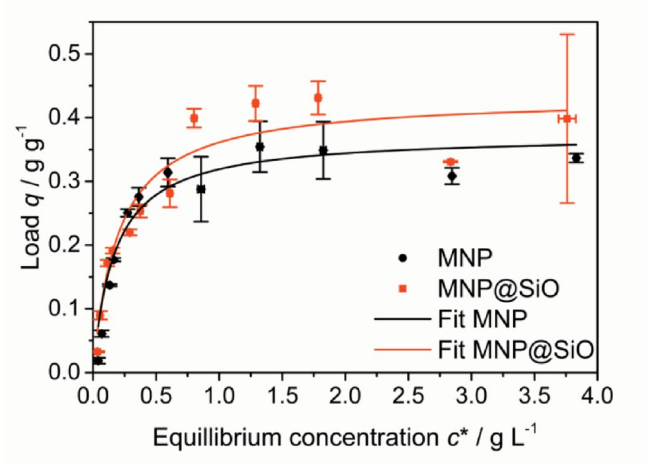

Figure 2. Adsorption isotherms at different cellulose concentrations with 1 g L^{-1} MNPs or MNP@SiO at 50 °C for 10 h. Error bars were derived from three incubation experiments and a photometric analysis in triplicate (± SD).

colloidal carrier materials before CEL immobilization yielded an increased binding capacity. Therefore, q_{max} values of 0.37 and 0.43 g g^{-1} could be reached for MNPs and MNP@SiO, respectively. This load is ten times higher than comparable nanocarrier systems and is, therefore, the basis of a high-performance enzyme catalysis process.[18] Furthermore, the binding constants K_D are in the same region for the MNPs (0.17 g L^{-1}) and MNP@SiO (0.20 g L^{-1}), which enables an excellent comparison of these nanoparticles when used as CEL carrier materials. In the following text, the CEL–particle composites are referred to as nano-biocatalysts (NBCs) and are distinguished according to the carrier material as NBC_{MNP} and NBC_{SiO}.

XRD data (Figure S1) show that there is no change in the crystal structure of the material and the crystallite size following the coating and functionalization procedures. However, the hydrodynamic diameter measured by dynamic light scattering (DLS), which is an important parameter for protein adsorption, changed significantly with the adsorption of CEL (Figure S6 b).[19] Although the hydrodynamic diameter for the MNPs is in the range of the particle diameter determined by TEM, MNP@SiO demonstrates a significantly larger diameter and a broader distribution (50 nm), which might be caused by aggregation with the silica coating. The addition of CEL to the nanoparticles leads to an increase in hydrodynamic diameter of 25 nm. This behavior can be connected to the protein corona formation of CEL around the particles.[20] The load of immobilized CEL was determined by simultaneous thermal analysis–mass spectrometry (STA–MS) of the dried samples. Results (Figure S7) show a distinct difference between the two carrier materials: Bare MNPs undergo a weight loss of around 2%, which is attributed to bound water. Also, carbon dioxide (CO_2) was detected in the MS, owing to adventitious carbon. Although a similar weight loss for MNP@SiO can be detected in this temperature region, no endothermic signal was observed at 500 °C. This emphasizes a comprehensive silica coating and, thus, protection from oxidative phase transition. Both NBCs show a weight loss of around 50% that can be attributed to to oxidation and desorption of CEL. Fragments could be detected as CO_2 signals by using MS (Figure S7). Both carrier materials demonstrate similar MS traces and exothermic desorption processes, as evidenced by differential scanning calorimetry (DSC) at around 300 and 750 °C. Although the desorption enthalpy for the MNP samples is around 5 mW mg^{-1} at 750 °C, the desorption enthalpy of MNP@SiO particles reaches a value of over 100 mW mg^{-1}. This behavior suggests a different adsorption mechanism of CEL on the surfaces of the respective carrier materials.

The immobilization of CEL on both carrier materials is further evidenced by XPS and ATR–IR (Figures S2–S4). XPS demonstrates a distinct increase in the C 1s region as well as the N 1s region for the NBCs (Figures S3 b and S3 d). The ATR–IR spectra exhibit typical amide bands at 1640 and 1515 cm^{-1}.[21] Furthermore, glycosylated protein sites are represented by bands at 1070 cm^{-1} (Figure S4).[22]

The enzymatic activity of NBCs was verified with a *p*-nitrophenol (*p*NP) assay. Compared to free CEL, the mass-specific relative activity was determined as 38 and 19% for NBC_{SiO} and NBC_{MNP}, respectively (Figure S8). This loss in activity plays a minor role in the described NBC systems, as the enzyme load is extremely high and considerable CEL conversion rates can be achieved. The discrepancy in the enzyme activity can be connected to different binding mechanisms of CEL on the differently charged particle surfaces.[23]

The high enzymatic activity of immobilized CEL and the convenient handling of the NBCs provide enormous opportunities for industrial applications. Furthermore, we could reach an excellent recyclability and enzyme stability over multiple cycles

of magnetic separation and NBC recovery. No leaching of enzyme was detected by photometric detection and the activity loss could be ascribed to the deficiency of particles, which was determined by using a phenanthroline assay. In a recovery study of ten cycles, the relative enzymatic activity remained high (Figure 3), but 26% (w/w) NBC_{SiO} and 12% (w/w) of the NBC_{MNP} was lost during the recycling (Figure S9). The recyclability is significantly higher than that observed for other nanocarrier systems, where only 20% of the enzyme activity could be sustained after ten cycles.[24]

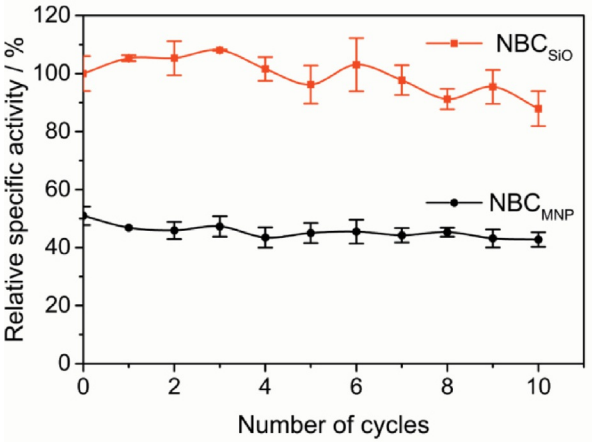

Figure 3. Relative specific activity of the NBCs over ten recycling steps; particle-loss corrected. Error bars were derived from a *p*NP assays conducted in triplicate and the photometric analysis of three samples for each assay (±SD).

This high recovery rate can be connected to the extraordinarily high saturation magnetization (M_S) for both NBC species. The M_S values in a magnetic field of 50000 Oe were 42 and 57 emu g^{-1} for NBC_{SiO} and NBC_{MNP}, respectively. Each of the carrier materials demonstrated superparamagnetic behavior at room temperature (Figure S10). A further positive aspect of CEL immobilization is the increase in long-term stability. After 30 days of storage, the relative enzymatic activity of the NBCs remained at 76%, whereas the free CEL solution only demonstrated 9% of its initial enzymatic activity. Analysis of pH and temperature stabilities demonstrated no significant improvement for the NBCs compared to free CEL (Figure S12).

Motivated by the ambitious goals of the biofuel sector, CEL was chosen for enzyme immobilization to upgrade cellulose-based ethanol to an economically competitive product. This study demonstrates the successful combination of the unique magnetic separation properties of cost-effective, easily producible MNPs as a carrier material with the key benefits of physical enzyme adsorption. The surface charge plays a critical role in the protein adsorption and influences the protein corona as well as the activity of bound enzymes. NBCs were prepared from bare MNPs and MNP@SiO. The presented NBC_{SiO} outperforms comparable systems in terms of enzyme loading and, beyond that, demonstrates high lifecycle stability and recyclability. Furthermore, the magnetic and mechanic properties of the support material offer the unique ability to separate the NBCs magnetically from a solid-containing process stream, for example, the insoluble lignin in cellulose hydrolysate, even in viscous media. As shown in the Supporting Information, the bare magnetite surface is electrostatically flexible and should also be able to serve as a carrier for other enzymes. A further improvement of these NBCs would be their application in solid-containing straw lysates and the immobilization of more active enzymes.

Experimental Section

All details about the synthesis, coating, functionalization, and analysis can be found in the Supporting Information.

Acknowledgements

H.-C.R. thanks the Bavarian Ministry of Economic Affairs and Media, Energy and Technology (Grant number 1340/68351/3/11) for financial support. S.P.S. is thankful for funding from the Federal Ministry of Education and Research (Grant number 031A173A). We appreciate support from the German Research Foundation (DFG) and the Technical University of Munich (TUM) in the framework of the Open-Access Publishing Program.

Keywords: enzyme catalysis · immobilization · magnetic separation · nano-biotechnology · nanomaterials

[1] a) A. Liese, L. Hilterhaus, *Chem. Soc. Rev.* **2013**, *42*, 6236–6249; b) P. Gallezot, *Chem. Soc. Rev.* **2012**, *41*, 1538–1558; c) *OECD-FAO Agricultural Outlook 2014–2023*, OECD, Paris, **2014**.
[2] R. DiCosimo, J. McAuliffe, A. J. Poulose, G. Bohlmann, *Chem. Soc. Rev.* **2013**, *42*, 6437–6474.
[3] M. C. R. Franssen, P. Steunenberg, E. L. Scott, H. Zuilhof, J. P. M. Sanders, *Chem. Soc. Rev.* **2013**, *42*, 6491–6533.
[4] L. Cao, *Curr. Opin. Chem. Biol.* **2005**, *9*, 217–226.
[5] U. T. Bornscheuer, *Angew. Chem. Int. Ed.* **2003**, *42*, 3336–3337; *Angew. Chem.* **2003**, *115*, 3458–3459.
[6] U. Bornscheuer, K. Buchholz, J. Seibel, *Angew. Chem. Int. Ed.* **2014**, *53*, 10876–10893; *Angew. Chem.* **2014**, *126*, 11054–11073.
[7] L. M. Rossi, N. J. S. Costa, F. P. Silva, R. Wojcieszak, *Green Chem.* **2014**, *16*, 2906.
[8] G.-X. Zhou, G.-Y. Chen, B.-B. Yan, *Biotechnol. Lett.* **2014**, *36*, 63–68.
[9] a) R. A. Sheldon, *Adv. Synth. Catal.* **2007**, *349*, 1289–1307; b) E. Katz, I. Willner, *Angew. Chem. Int. Ed.* **2004**, *43*, 6042–6108; *Angew. Chem.* **2004**, *116*, 6166–6235; c) L. Betancor, H. R. Luckarift, *Trends Biotechnol.* **2008**, *26*, 566–572; d) S. Datta, L. R. Christena, Y. R. S. Rajaram, *Biotechnology* **2013**, *3*, 1–9.
[10] U. Hanefeld, L. Gardossi, E. Magner, *Chem. Soc. Rev.* **2009**, *38*, 453–468.
[11] O. Kudina, A. Zakharchenko, O. Trotsenko, A. Tokarev, L. Ionov, G. Stoychev, N. Puretskiy, S. W. Pryor, A. Voronov, S. Minko, *Angew. Chem. Int. Ed.* **2014**, *53*, 483–487; *Angew. Chem.* **2014**, *126*, 493–497.
[12] A.-H. Lu, E. L. Salabas, F. Schüth, *Angew. Chem. Int. Ed.* **2007**, *46*, 1222–1244; *Angew. Chem.* **2007**, *119*, 1242–1266.
[13] S. Shylesh, V. Schünemann, W. R. Thiel, *Angew. Chem. Int. Ed.* **2010**, *49*, 3428–3459; *Angew. Chem.* **2010**, *122*, 3504–3537.
[14] P. Fraga García, M. Brammen, M. Wolf, S. Reinlein, M. Freiherr von Roman, S. Berensmeier, *Sep. Purif. Technol.* **2015**, *150*, 29–36.
[15] H.-C. Roth, S. P. Schwaminger, M. Schindler, F. E. Wagner, S. Berensmeier, *J. Magn. Magn. Mater.* **2015**, *377*, 81–89.
[16] H.-C. Roth, A. Prams, M. Lutz, J. Ritscher, M. Raab, S. Berensmeier, *Chem. Eng. Technol.* **2016**, *39*, 469–476.
[17] P. Innocenzi, *J. Non-Cryst. Solids* **2003**, *316*, 309–319.
[18] M. Misson, H. Zhang, B. Jin, *J. R. Soc. Interface* **2015**, *12*, 20140891.

[19] P. Fraga García, M. Freiherr von Roman, S. Reinlein, M. Wolf, S. Berensmeier, *ACS Appl. Mater. Interfaces* **2014**, *6*, 13607 – 13616.
[20] S. Tenzer, D. Docter, J. Kuharev, A. Musyanovych, V. Fetz, R. Hecht, F. Schlenk, D. Fischer, K. Kiouptsi, C. Reinhardt, K. Landfester, H. Schild, M. Maskos, S. K. Knauer, R. H. Stauber, *Nat. Nanotechnol.* **2013**, *8*, 772 – 781.
[21] V. Zlateski, R. Fuhrer, F. M. Koehler, S. Wharry, M. Zeltner, W. J. Stark, T. S. Moody, R. N. Grass, *Bioconjugate Chem.* **2014**, *25*, 677 – 684.
[22] M. Khajehpour, J. L. Dashnau, J. M. Vanderkooi, *Anal. Biochem.* **2006**, *348*, 40 – 48.
[23] S. P. Schwaminger, P. Fraga García, G. K. Merck, F. A. Bodensteiner, S. Heissler, S. Günther, S. Berensmeier, *J. Phys. Chem. C* **2015**, *119*, 23032 – 23041.
[24] J. Jordan, C. Theegala, *Biomass Convers. Biorefin.* **2014**, *4*, 25 – 33.

Received: March 24, 2016
Published online on April 29, 2016

